Augmented Linear Quadratic Tracker for Enhanced Output-Voltage Control of DC-DC Buck Converter

Omer Saleem*, Mohsin Rizwan, Muaaz Ahmad***

** Department of Electrical Engineering, National University of Computer and Emerging Sciences, Lahore, Pakistan (e-mail: omer.saleem, l144442@nu.edu.pk)*
*** Department of Mechatronics and Control Engineering, University of Engineering and Technology, Lahore, Pakistan (e-mail: mohsin.rizwan@uet.edu.pk)*

Abstract: This paper presents a methodic approach to synthesize a robust affine state-feedback controller to enhance the output-voltage tracking control performance of a DC-DC buck converter circuit. The proposed control scheme primarily utilizes a conventional linear-quadratic-tracker (LQT) that renders optimal control decisions based on the state-feedback of output-voltage and inductor-current. Additionally, it employs a feed-forward control term to track the time-varying reference voltage trajectories. Despite its optimality, the LQT lacks robustness in eliminating the steady-state errors and compensating the effects of bounded exogenous disturbances that are caused by high-frequency noises, load-step transients, and modeling errors. In this research, the conventional LQT is equipped with auxiliary tools to dynamically compensate the aforementioned parametric uncertainties. The existing state-space model of the system is augmented with an additional integral-of-error state-variable to eliminate the steady-state fluctuations in output-voltage response. The controller is also retrofitted with a self-tuning capacitor-current control term in order to emulate and deliver the derivative control effort. It rejects the disturbances, compensates the hysteresis effect rendered by the parasitic impedances, and improves the error convergence-rate of the response. The proposed augmented tracking controller is rigorously analyzed via experimental tests to validate its effectiveness.

Keywords: Buck converter, linear quadratic tracker, integral control, capacitor-current, self-tuning control.

1. INTRODUCTION

The buck converter is a static power electronic converter that reduces a direct-current (DC) voltage source from a higher level to a lower level. The DC-DC converters are widely used in adjustable motor speed drives, electric vehicles, uninterrupted power supplies, communication equipment, ceiling elevators, computer systems, telephone sets, and inverters, etc (Tahri et al., 2012; Ghosh and Banerjee, 2015). The regulated output-voltage (v_o) response of the buck converter is prone to be degraded by the unprecedented fluctuations in the load impedance or the unregulated DC input voltage (v_{in}). However, this problem is normally solved with the aid of a negative-feedback closed-loop control system in the circuit. Where in, the v_o is continuously compared with the reference voltage (v_{ref}), and the resulting error dynamics are used to adjust the duty-cycle (d) of the active switch in the circuit to stabilize the v_o at the desired reference.

A plethora of linear and nonlinear controllers have been proposed in the literature to enhance the voltage tracking control and regulation capability of the buck converter (Lindiya et al., 2012; Pedroso et al., 2013). The proportional-integral-derivative controllers are widely used in the industry owing to their simplicity, robustness and model-free nature (Jalilyand et al., 2010; Seshagiri et al., 2016; Mehendran and Ramabadran, 2016). However, finding a trivial set of controller gains that yield optimal control performance is a cumbersome process. The pole-placement techniques have also been rigorously investigated (Benzaouia et al., 2016). But, as mentioned earlier, appropriate placement of the poles to achieve optimal time-domain control performance is a difficult and time-consuming task. Other model free control techniques that have been proposed in the literature are fuzzy logic controllers (Kumar et al., 2013; Boutouba et al., 2017; Lian et al., 2017). These intelligent controllers require heuristically fabricated logical rule bases. The artificial synthesis of rule-base hinders the fuzzy controllers to optimally cater the nonlinearities associated with the system. The fractional-order PID controllers introduce additional hyper-parameters to increase the degrees-of-freedom and flexibility of controller design (Bhaumik et al., 2016; Zhu et al., 2014). However, the parameter optimization is a computationally expensive task. Other mentionable control techniques include back-stepping control and sliding mode control (McIntyre et al., 2015; Qi et al., 2018).

The state-space controllers can deliver optimal control decisions, since they utilize the full state-feedback of the system along with its linear mathematical model (Lakshmi and Raja, 2014; Akter et al., 2015). Extensive research has been done on linear quadratic regulators as an optimal voltage control scheme for buck converters (Moreira et al., 2011; Lindiya et al., 2016). However, despite their optimality, the conventional LQRs severely lack in robustness against dynamic variations in the reference trajectory, high frequency noise, load-step changes, line-voltage fluctuations, steady-state errors, modeling errors, and exogenous disturbances (Cui et al., 2014). Several control schemes have been proposed in the literature to enhance the reference trajectory tracking performance of the buck converters (Pedroso et al., 2013; Spinu et al., 2014; Tan et al., 2014; Karanjkar et al., 2014; Lee et al., 2016). However, they require extensive computational resources. The conventional LQRs are normally equipped with a feed-forward control term in order to accurately track the time-varying trajectories. Such controllers are referred to as the linear quadratic trackers (LQT), (Kiumarsi et al., 2015; Modares et al., 2014; He et al., 2017). The suppression of the modeling-uncertainties and other disturbances still remains a major concern for the LQTs (Ghartemani et al., 2011).

In this research, the robustness of a conventional LQT is enhanced by augmenting it with additional controlling tools. Firstly, an auxiliary state-variable regarding the integral-or-error in v_o is introduced in the existing state-space model (Ruderman et al., 2008). The proposed augmentation eliminates the steady-state errors and damps the unnecessary overshoots, undershoots, and oscillations. Secondly, the existing control is retrofitted with a derivative control term in order to improve the transitional-times and error-convergence rate of the response. Furthermore, it significantly improves the disturbance rejection capability of the system, and compensates the damping effect rendered by the integral term. However, simultaneously, it also amplifies the high frequency noise. Hence, in this paper, the state-variable regarding the derivative-of-v_o is replaced with the capacitor-current (i_c) term in the control law (Kapat and Krein, 2012; Kapat and Krein, 2012). This augmentation also attenuates the effects of hysteresis rendered by the parasitic impedances. Once the LQT is equipped with the auxiliary components, the augmented tracking controller (ATC) is experimentally tested and the results are analyzed to justify its efficacy.

The rest of the paper is organized as follows: Section 2 presents the theoretical background and the mathematical model of the converter. The conventional LQR is describes in Section 3. The proposed controller is synthesized in Section 4. The experimental comparison of the proposed controller with the conventional LQR is provided in Section 5. The paper is concluded in Section 6.

2. EXPERIMENTAL SETUP

The buck convertor is a switch-mode power supply that reduces and regulates a given DC input voltage source to a desired level. The high-frequency switching transistor in the converter circuit chops down the DC input voltage into a rectangular waveform. This rectangular waveform is fed to a low-pass filter formed by the inductor-capacitor network which only allows the DC component (average value) of the waveform to pass though. The output voltage of convertor, given by (1), can be regulated by varying the duty-cycle ratio (d) of the transistor. The duty-cycle ratio is given by (2).

$$v_o = d \times v_{in} \tag{1}$$

$$d = \frac{t_{on}}{t_{on} + t_{off}} \tag{2}$$

where, t_{on} and t_{off} refers to the on-time and off-time of switching period, respectively. In case of any fluctuations in the load-resistance (R) or v_{in}, the negative-feedback controller changes the duty-cycle of the switching period in order to maintain the v_o at the reference value. During the on-time of switch, the entire current from the input passes through the capacitor and the load-resistor, while charging the inductor in its path. The diode stays reverse biased during this time. During the off-time of switch, the input supply to the remaining circuit is cut-off. However, the diode is forward-biased which closes the circuit loop and allows the inductor to discharge through the capacitor and load-resistor (Mohan et al., 2007). The hardware setup as well as the mathematical model of the DC-DC buck convertor is presented in the following sub-sections.

2.1 Hardware setup

The circuit diagram of the buck convertor is shown in Fig. 1. The output-voltage (v_o) is measured with the aid of a voltage sensor. The inductor-current (i_L) is measured via a shunt resistor of 0.01 Ω, 5.0W. The real-time analog measurements of the states are fed to a 32-bit embedded microcontroller (Antão et al., 2014). The microcontroller filters and digitizes the acquired sensor-data at a sampling frequency of 1000 Hz. The microcontroller serially transmits the conditioned sensor-data, at 9600 bps, to the control system that is implemented in a MATLAB based computer application (Duong et al., 2017; Bagewadi and Dambhare, 2017). The control system generates optimal correctional commands based on the variations in state-feedback. These commands are serially communicated back to the microcontroller where they are transformed into high-frequency pulse-width modulated (PWM) signals. Eventually, the PWM commands are used to drive the MOSFET (metal oxide surface field effect transistor) switch in the convertor circuit via a dedicated optically isolated PWM amplifier. In this research, the transistor is switched on and off at a frequency of 100 kHz. The above-mentioned computer application is also used for the graphically visualization of the state variations in real-time.

2.2 Mathematical model

The state-space model of a linear dynamical system is given by (3) and (4).

$$\dot{x}(t) = \boldsymbol{A}x(t) + \boldsymbol{B}u(t) \tag{3}$$

$$y(t) = \boldsymbol{H}x(t) + \boldsymbol{F}u(t) \tag{4}$$

where, *x(t)* is the state-vector, *y(t)* is the output-vector, *u(t)* is the control input signal, ***A*** is the system-transition matrix, ***B*** is the input vector, ***H*** is the output vector, and ***F*** is the feed-forward matrix. The state-vector and the control input of the buck converter are defined in (5).

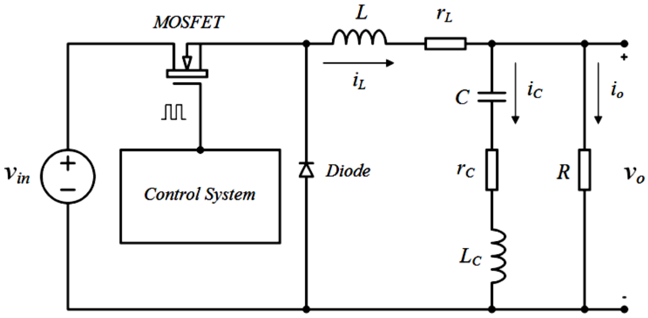

Fig. 1. Buck converter circuit

$$x(t) = [v_o(t) \quad i_L(t)]^T, \qquad u(t) = d(t) \tag{5}$$

where, $d(t)$ is the instantaneous value of duty-cycle. The averaged mathematical model of the converter is experimentally identified. The matrices $\boldsymbol{A}$, $\boldsymbol{B}$, $\boldsymbol{H}$, and $\boldsymbol{F}$ of the buck converter's state-space model are defined in (6), (Kapat and Krein, 2010).

$$\boldsymbol{A} = \begin{bmatrix} -\frac{1}{C(R+r_c)} & \frac{R}{C(R+r_c)} \\ -\frac{R}{L(R+r_c)} & -\frac{(r_L + r_c||R)}{L} \end{bmatrix}, \qquad \boldsymbol{B} = \begin{bmatrix} 0 \\ \frac{v_{in}}{L} \end{bmatrix},$$

$$\boldsymbol{H} = [1 \quad 0], \qquad \boldsymbol{F} = 0 \tag{6}$$

The design parameters of the buck converter circuit, used in this research, are identified in Table 1.

3. LINEAR QUADRATIC TRACKER

The linear quadratic tracker (LQT) is a model-based tracking control mechanism that uses the affine state-feedback to deliver optimal control effort. The LQT consists of the usual state-feedback of the linear dynamical system along with additional feed-forward control term. It minimizes the quadratic performance index, given by (7), to generate optimal control decisions (Lewis et al., 2012).

$$J = \frac{1}{2}\int_0^T \left(\boldsymbol{H}x - v_{ref}\right)^T \boldsymbol{Q}\left(\boldsymbol{H}x - v_{ref}\right) + u^T \boldsymbol{R} u \, dt \tag{7}$$

where, $\boldsymbol{Q}$ and $\boldsymbol{R}$ are the intermediate-state and control weighting matrices, respectively.

Table 1. Design parameters of buck-converter circuit

Parameters	Symbol	Values
Load-resistance	R	10 Ω
Inductance	L	330 μH
Capacitance	C	1000 μF
ESR of capacitor	r_c	0.08 Ω
ESR of inductor	L_c	0.1 μH
ESL of capacitor	r_L	0.07 Ω
Input voltage	v_{in}	30 V
Output Power	P_{out}	100 W

They are chosen such that; $Q = Q^T \geq 0$ and $R = R^T > 0$. Owing to the quadratic nature of the cost function, the control signal, d, is proportional to the square of variations in the states. Thus, if the state-variations are large; the minimization and, hence, the convergence-rate is faster. The weighting matrices used in this research are given by (8).

$$\boldsymbol{Q} = \begin{bmatrix} 1 & 0 \\ 0 & 1 \end{bmatrix}, \qquad \boldsymbol{R} = 10 \tag{8}$$

The optimal affine control decisions are evaluated via the expression given by (9).

$$d(t) = -\boldsymbol{K}x(t) + K_{ff}r(t) \tag{9}$$

$$\text{where}, \boldsymbol{K} = \boldsymbol{R}^{-1}\boldsymbol{B}^T\boldsymbol{P} \tag{10}$$

$$\text{and}, K_{ff} = -\boldsymbol{R}^{-1}\boldsymbol{B}^T((\boldsymbol{A} - \boldsymbol{B}\boldsymbol{K})^{\mathrm{T}})^{-1}\boldsymbol{H}^T\boldsymbol{Q} \tag{11}$$

The gain vector, $\boldsymbol{K}$, helps to relocate the open-loop poles of the system to synthesize an optimal controller. The optimal Kalman gain vector depends on a symmetric positive definite matrix $\boldsymbol{P}$ that is evaluated for the given system by solving the Algebraic Riccati Equation, shown in (12).

$$\boldsymbol{A}^T\boldsymbol{P} + \boldsymbol{P}\boldsymbol{A} - \boldsymbol{P}\boldsymbol{B}\boldsymbol{R}^{-1}\boldsymbol{B}^T\boldsymbol{P} + \boldsymbol{H}^T\boldsymbol{Q}\boldsymbol{H} = 0 \tag{12}$$

In order to incorporate optimizing the trajectory tracking response, a feed-forward (*ff*) control term is added to the LQT control law. This term compensates the dynamic changes in the reference trajectory. The feed-forward gain (K_{ff}), shown in (11), depends on the output of the adjoint of the closed-loop plant when driven by $v_{ref}(t)$, (Lewis et al., 2012). Owing to the system description, provided in the previous section, the optimal state-feedback gain vector ($\boldsymbol{K}$) and the feed-forward gain (K_{ff}) are given in (13) and (14), respectively.

$$\boldsymbol{K} = [K_{v_o} \quad K_{i_L}] = [0.2403 \quad 0.1102] \tag{13}$$

$$K_{ff} = -0.306 \tag{14}$$

4. PROPOSED CONTROL SCHEME

This section presents the synthesis of the proposed state-feedback control scheme. The conventional LQT is at the heart of the proposed controller. However, it is equipped with two additional controlling mechanisms in order to improve its overall performance in the time-domain. Firstly, the existing state-space model of the motor is modified by retrofitting it with an auxiliary state-variable regarding the integral-of-error. Secondly, the control system is also augmented with an active disturbance rejection controller. The mathematical derivation of the proposed control scheme is as follows.

4.1 Auxiliary integral state-variable

In order to improve the steady-state performance of the control scheme, the existing LQT architecture is retrofitted with an auxiliary control term that delivers the correctional efforts based on the integral-of-error in v_o. The augmentation of integral controller effectively eliminates the steady-state errors, inhibits the overshoots (or undershoots), and damp the oscillations. The integral of error is given by (15).

$$\varepsilon(t) = \int_{0}^{t} e(\tau)\, d\tau \tag{15}$$

such that,

$$e(t) = v_{ref}(t) - v_o(t) \tag{16}$$

With the introduction of the integral-of-error (ε) as an additional state-variable in the existing state-space model, the augmented controller is denoted as the linear-quadratic-integral-tracker (LQIT). The augmented state-vector is given by (17).

$$\hat{x}(t) = [v_o(t) \quad i_L(t) \quad \varepsilon(t)]^T \tag{17}$$

The revised state-space model is given by (18).

$$\begin{bmatrix} \dot{v_o} \\ \dot{i_L} \\ \dot{\varepsilon} \end{bmatrix} = \begin{bmatrix} -\dfrac{1}{C(R+r_c)} & \dfrac{R}{C(R+r_c)} & 0 \\ -\dfrac{R}{L(R+r_c)} & -\dfrac{(r_L + r_c||R)}{L} & 0 \\ -1 & 0 & 0 \end{bmatrix} \begin{bmatrix} v_o \\ i_L \\ \varepsilon \end{bmatrix} + \begin{bmatrix} 0 \\ \dfrac{v_{in}}{L} \\ 0 \end{bmatrix} d + \begin{bmatrix} 0 \\ 0 \\ 1 \end{bmatrix} v_{ref} \tag{18}$$

The output vector, H, is also modified according to (19).

$$H = [1 \quad 0 \quad 0] \tag{19}$$

The $\boldsymbol{Q}$ matrix is augmented with a small weight for the ε. The updated $\boldsymbol{Q}$ matrix is given by (20).

$$\boldsymbol{Q} = \begin{bmatrix} 1 & 0 & 0 \\ 0 & 1 & 0 \\ 0 & 0 & 0.001 \end{bmatrix} \tag{20}$$

Consequently, the LQIT control law is given by (21).

$$d(t) = -\widehat{\boldsymbol{K}}\hat{x}(t) + \widehat{K}_{ff} r(t) \tag{21}$$

The augmented Kalman gain vector ($\widehat{\boldsymbol{K}}$) and the feed-forward gain ($\widehat{K}_{ff}$) are given by (22) and (23), respectively.

$$\widehat{\boldsymbol{K}} = [K_{v_o} \quad K_{i_L} \quad K_{\varepsilon}] = [0.2407 \quad 0.1108 \quad -0.014] \tag{22}$$

$$\widehat{K}_{ff} = 0 \tag{23}$$

The feed-forward gain of the LQIT is zero. It is justified because the expression of ε, given by (15), already includes the dynamic variations of v_{ref}, apart from eliminating the steady-state fluctuations.

4.2 Disturbance rejection controller

The LQIT is equipped with a disturbance rejection controller (DRC) as well. It serves to compensate the effects of bounded exogenous disturbances that are caused by the modeling uncertainties, step-changes in load-resistances, and transients in v_{in}. A control term acting directly on the derivative-of-error in v_o is needed. Apart from enhancing the controller's robustness against the aforementioned disturbances, the derivative-of-error in v_o also enhances its phase margin and global asymptotic convergence. This feature is particularly useful in tracking the time-varying trajectories (Saleem et al., 2017), and countering the damping effects introduced by the auxiliary integral control term.

However, the derivative action has an inherent problem. The derivative operator inevitably amplifies the high frequency noise in the closed-loop system. The parasitic impedance; namely, equivalent series resistance (ESR) and equivalent series inductance (ESL) of the capacitor, also tend to impede the derivative controller performance. This phenomenon leads to large overshoots (or undershoots) during large-signal transients and abrupt bipolar fluctuations during small-signal transients (Kapat and Krein, 2012). Enhancing the derivative computation with the aid of extended-state-observes or tracking differentiators is a cumbersome and computationally expensive process.

A tangible solution is to directly measure and control the capacitor-current, instead of computing the derivative-term. The practical model of the output capacitor is given by (24).

$$\frac{dv_o(t)}{dt} = L_c \frac{d^2 i_c(t)}{dt^2} + r_c \frac{di_c(t)}{dt} + \frac{i_c(t)}{C} \tag{24}$$

With the inclusion of random disturbances in the capacitor model, the capacitor current (i_c) of the buck convertor can be expressed according to (25).

$$i_c(t) \approx \frac{r_c}{r_c C - L_c}\left(e^{\frac{-t}{r_c C}} - e^{\frac{-r_c t}{L_c}}\right) C \left(\frac{dv_o(t)}{dt}\right) \tag{25}$$

If the value of parasitics (ESR and ESL) is negligibly small, then i_c becomes equal to $C\left(\frac{dv_o}{dt}\right)$. Therefore, instead of computing the derivative of v_o, the proposed scheme directly uses the i_c. The instantaneous variations in i_c are measured with the aid of a shunt power resistor of 0.01 Ω (less than the value of capacitor's ESR). It renders insignificant effect on the closed-loop bandwidth and stability (Kapat and Krein, 2010). Additionally, it reinforces the feed-forward information regarding the real-time variations in the load-current and i_L. Finally, it yields effective hysteresis compensation control as well. The disturbance rejection controller is given by (26).

$$d_{drc}(\mathrm{t}) = -K_d i_C(\mathrm{t}) \tag{26}$$

where, K_d is the derivative gain. The introduction of d_{drc} controller with a fixed derivative gain may not be very beneficial. Although it improves the transient response of the system, but, it also inevitably leads to persistent fluctuations in the steady-state error. This phenomenon counters the control action yielded by the auxiliary integral controller. Hence, the derivative gain is adaptively modulated by a nonlinear function of error. Several options of nonlinear functions are proposed in literature for the adaptive self-tuning of the controller gains (Seraji, 1998; Guo et al., 2012; Saleem and Omer, 2017). The proposed technique requires a smooth, symmetrical, and differentiable function. Therefore, a hyperbolic secant function depending on the instantaneous value of error (e) is used (Isayed and Hawwa, 2007). The adaptive derivative gain function is given by (27).

$$K_d = 0.05 + 1.84(1 - sech(\alpha \times e)) \tag{27}$$

Where, α is the variance of the function. In this research, its value is heuristically selected to be 2.71 via trial-and-error method. The waveform of the derivative-gain function is shown in Fig. 2. The waveform clearly manifests that the derivative gain will render major contribution in overall control decision when the error is large (during transients). The gain gradually decreases as the error reduces, or as the response converges towards the reference. The gain becomes negligible when the error is small, or as the system settles in the steady-state.

4.3 Augmented tracking controller

With the addition of the aforementioned individual control mechanisms in the existing LQT architecture, the resulting augmented tracking controller (ATC) is given by (27).

$$d(t) = -\widehat{\boldsymbol{K}}\hat{x}(\mathrm{t}) + \widehat{K}_{ff} v_{ref}(\mathrm{t}) + d_{drc}(\mathrm{t}) \tag{27}$$

The control law in (27) can be re-written according to the expression given by (28).

$$d(t) = -\begin{bmatrix} K_{v_o} & K_{i_L} & K_{\varepsilon} \end{bmatrix} \begin{bmatrix} v_o \\ i_L \\ \varepsilon \end{bmatrix} - K_d i_C(\mathrm{t}) \tag{28}$$

The block diagram of the ATC architecture is given in Fig. 3.

5. TESTS AND RESULTS

The voltage regulation and control performances of the LQT, LQIT, and ATC are comparatively analyzed by subjecting them to the following five ‘hardware-in-the-loop’ experimental test-cases.

Test A: The performance of the aforementioned control schemes in regulating the v_o, at a step- reference of +10.0 V, is tested under normal conditions. The resulting variations in v_o, exhibited by each of the three controllers (LQT, LQIT, and ATC), are shown in Fig. 4, 5, and 6, respectively.

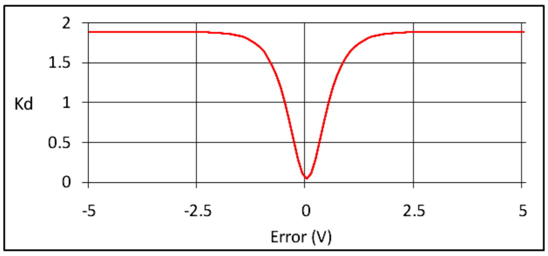

Fig. 2. Waveform of derivative-gain function

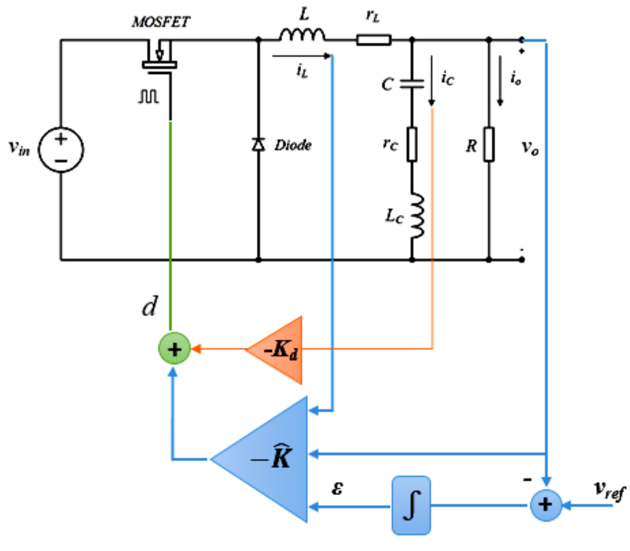

Fig. 3. Augmented tracking controller (ATC)

The analysis of the graphical results clearly validates the superior performance of the ATC. The auxiliary integral state-feedback minimizes the steady state error and damps the overshoot. The self-tuning i_c controller significantly improves the transient response as compared to that of LQT and LQIT. The corresponding variations incurred in the derivative-gain are shown in Fig. 7.

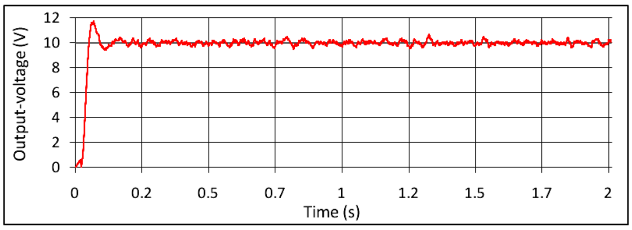

Fig. 4. Step-response of LQT

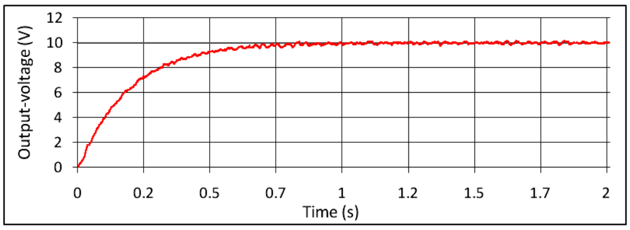

Fig. 5. Step-response of LQIT

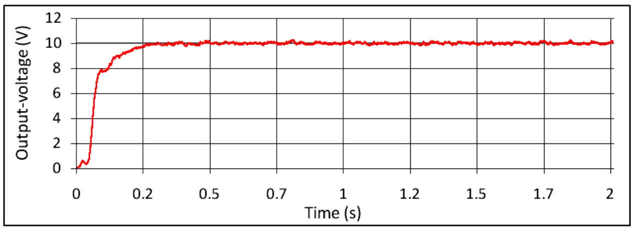

Fig. 6. Step-response of ATC

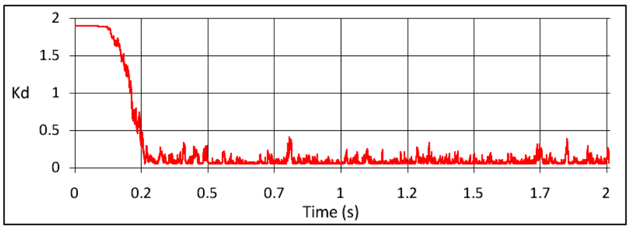

Fig. 7. Variations in K_d under step-reference

Test B: The robustness of each controller is tested under load-disturbance conditions. The abrupt variations occurring in the response, for a 50% incremental load-step, are illustrated in Figure 8, 9, and 10. The ATC effectively rejects the impulsive disturbance, while maintaining a quick convergence rate. The variations in K_d are shown in Fig. 11.

Test C: The robustness of each controller is tested by abruptly decreasing the input voltage from 30 V to 25 V. The corresponding perturbations exhibited by the response of v_o are illustrated in Fig. 12, 13, and 14, respectively. The ATC effectively damps the oscillations caused by the fluctuations in v_{in}. The variations in K_d are shown in Fig. 15.

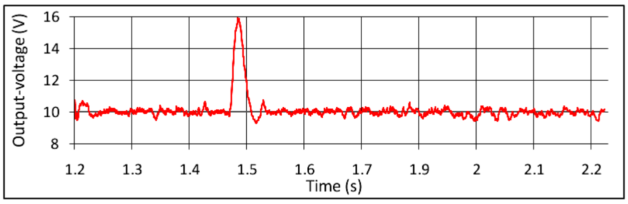

Figure 8. Response of LQT under load-step disturbance

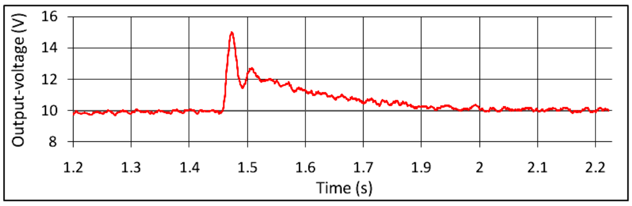

Fig. 9. Response of LQIT under load-step disturbance

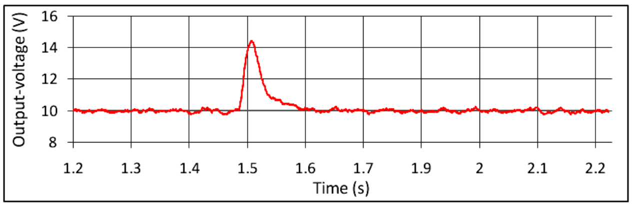

Fig. 10. Response of ATC under load-step disturbance

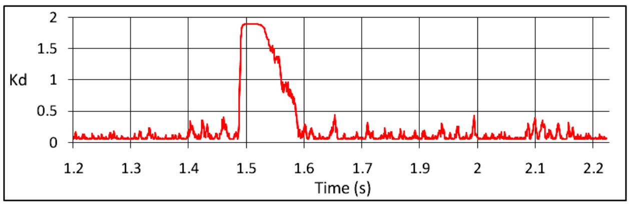

Fig. 11. Variations in K_d under load-step disturbance

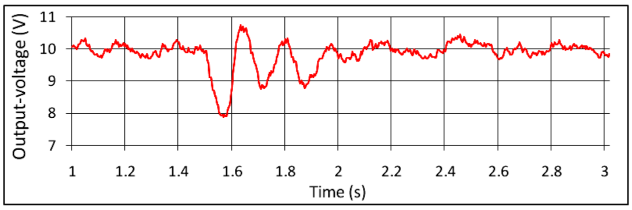

Fig. 12. Response of LQT under input-voltage disturbance

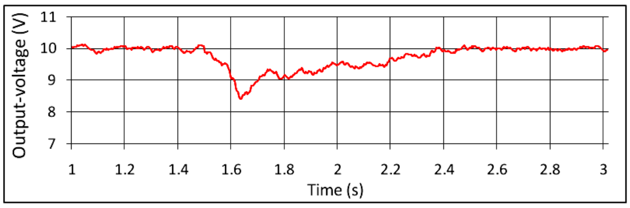

Fig. 13. Response of LQIT under input-voltage disturbance

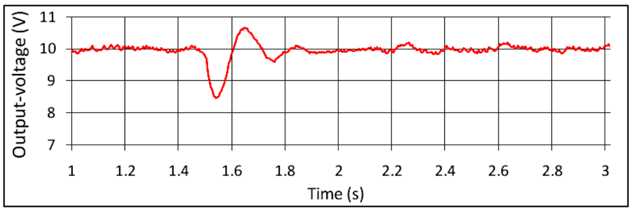

Fig. 14. Response of ATC under input-voltage disturbance

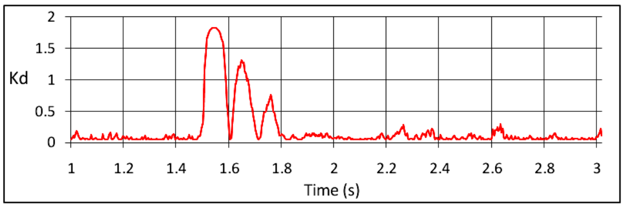

Fig. 15. Variations in K_d under input-voltage disturbance

Test D: The voltage-trajectory tracking performance of the controllers is tested by applying square-wave reference signal. The reference signal switches between discrete reference voltage-levels of +16.0 V and +4.0 V after a regular interval of 1.25 s. The corresponding response of v_o, under the influence of each of the three controllers, is illustrated in Fig. 16, 17, and 18, respectively. The ATC tracks the abrupt variations in the reference voltage with a significantly better transient and steady-state response. The corresponding variations in K_d are shown in Fig. 19.

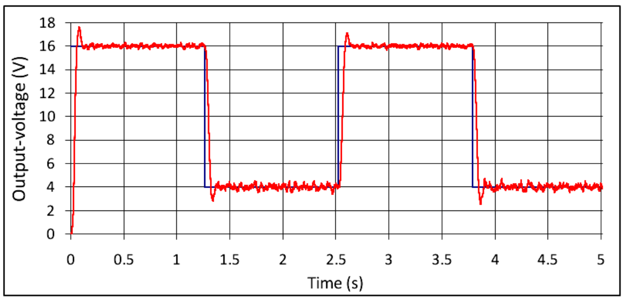

Fig. 16. Square-wave tracking response of LQT

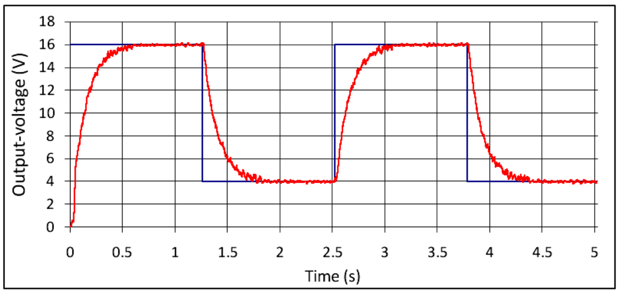

Fig. 17. Square-wave tracking response of LQIT

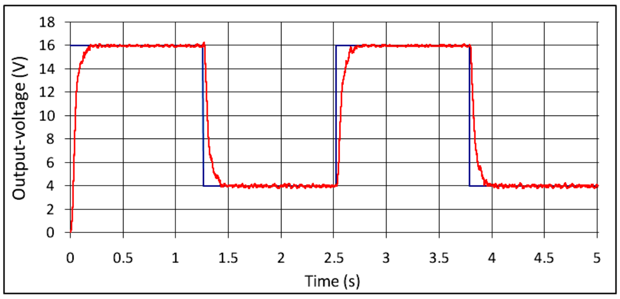

Fig. 18. Square-wave tracking response of ATC

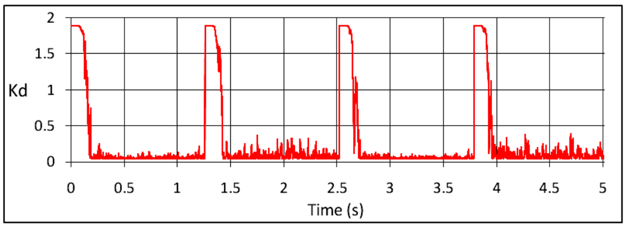

Fig. 19. Variations in K_d under square-wave tracking

Test E: The voltage-trajectory tracking performance of the controllers is tested by applying triangular reference input signal. The reference signal oscillates between +4.0 V and +16.0V. The oscillation frequency of the reference trajectory is 0.4 Hz. The corresponding perturbations exhibited by the response of v_o, under the influence of each of the three controllers, are illustrated in Figure 20, 21, and 22, respectively. The graphical responses validate the superiority of the trajectory tracking performance exhibited by ATC over the LQT and LQIT. The LQT exhibits significant tracking error. The LQIT shows a constant time-lag of 0.1 s while tracking the trajectory. The ATC precisely tracks the trajectory with negligible lag and minimum tracking error. The corresponding variations in K_d are shown in Fig. 23.

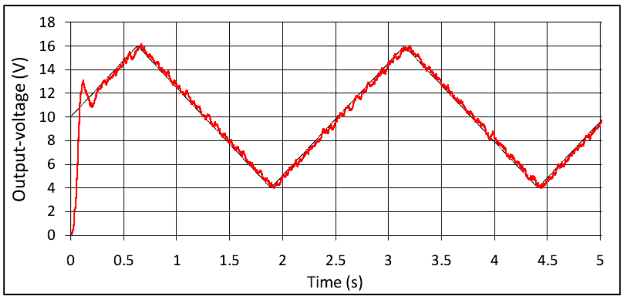

Fig. 20. Triangular-wave tracking response of LQT

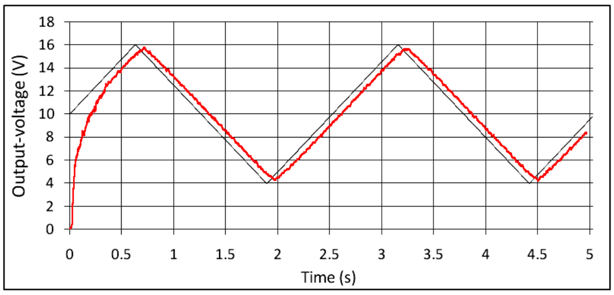

Fig. 21. Triangular-wave tracking response of LQIT

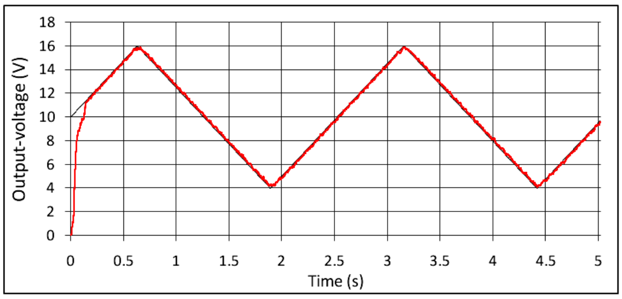

Fig. 22. Triangular-wave tracking response of ATC

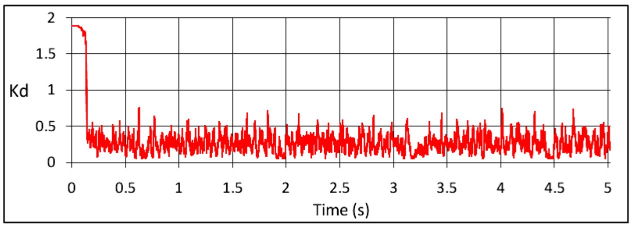

Fig. 23. Variations in K_d under triangular-wave tracking

The comparative performance assessment of the test results is summarized in Table 2. The responses rendered by each controller, for each test, are analyzed in terms of the rise-time (t_r), over-shoot or undershoot (M_p), settling-time (t_s), and root-mean-square of the steady-state error (e_{ss}).

Table 2. Summary of test results

Test	Controller	t_r (s)	M_p (%)	t_s (s)	e_{ss} (V)
A	LQT	0.09	17.45	0.13	0.85
	LQIT	0.49	0.01	0.71	0.13
	ATC	0.18	0.06	0.20	0.16
B	LQT	-	60.0	0.06	-
	LQIT	-	49.8	0.44	-
	ATC	-	44.3	0.11	-
C	LQT	-	21.1	0.49	-
	LQIT	-	15.2	0.83	-
	ATC	-	13.6	0.31	-
D	LQT	0.11	12.42	0.18	0.88
	LQIT	0.50	0.01	0.68	0.18
	ATC	0.20	0.04	0.23	0.17
E	LQT	0.09	15.56	0.29	0.79
	LQIT	0.49	0.01	-	1.12
	ATC	0.18	0.04	0.20	0.16

6. CONCLUSION

This paper presents an augmented affine state-feedback control scheme to robustify the output-voltage regulation and tracking control of a DC-DC buck converter. Apart from improving the trajectory tracking performance, the ATC significantly enhances the system's robustness against bounded exogenous disturbances. Furthermore, it also improves the error convergence-rate, of the system and effectively minimizes its steady-state (or tracking) error. The conventional LQT is employed as a state-space controller and it is equipped with two additional controlling tools to achieve the desired performance objectives. The summary of results, presented in Table 2, completely validates the efficacy rendered by the proposed augmentations in the control mechanism. Despite the evident performance enhancement yielded by the proposed controller, there is still a lot of room for future enhancements. Firstly, the LQT can be replaced by other model-based controllers; such as, model-predictive-controller and linear-quadratic-gaussian-tracker etc. Secondly, other self-tuning mechanism can be investigated to adaptively tune the derivative-gain. Thirdly, different meta-heuristic or gradient-based optimization techniques can be investigated to optimally select the Q and R weighting matrices of the LQ cost function. Finally, the proposed control mechanism can also be applied to regulate and control the output-voltage of other DC-DC switch-mode power electronic converters; such as, Cuk, Sepic, or Zeta converter.

REFERENCES

Akter, P., Uddin, M., Mekhilef, S., Tan, N.M.L., and Akagi, H. (2015). Model predictive control of bidirectional isolated DC–DC converter for energy conversion system. *International Journal of Electronics*, 102(8), pp. 1407-1427.

Antão, R., Mota, A., and Martins, R.E. (2014). Adaptive control of a buck converter with an ARM Cortex-M4. In: *Proceedings of 2014 16th International Power Electronics and Motion Control Conference and Exposition*. Antalya, Turkey, pp. 359-364.

Bagewadi, M.D., and Dambhare, S.S. (2017). A novel hybrid converter derived from buck-boost circuit for standalone applications. In: *Proceedings of 2017 19th European Conference on Power Electronics and Applications*, Warsaw, Poland, pp. 1-8.

Benzaouia, A., Soliman, H.M., Saleem, A. (2016). Regional pole placement with saturated control for DC-DC buck converter through Hardware-in-the-Loop. *Transactions of the Institute of Measurement and Control*, 38(9), pp. 1041-1052

Bhaumik, A., Kumar, Y., Srivastava, S., Islam, S.M. (2016). Performance studies of a separately excited DC motor speed control fed by a buck converter using optimized PIλDµ controller. In: *Proceedings of 2016 International Conference on Circuit, Power and Computing Technologies*, Nagercoil, India, pp. 1-6.

Boutouba, M., El-Ougli, A., Miqoi, S., and Tidhaf, B. (2017). Intelligent control for voltage regulation system via DC-DC Converter using Raspberry Pi 2 board. *WSEAS Transactions on Electronics*, 8, pp. 41-47.

Cui, H., Yang, J., and Li, S. (2014). Nonlinear disturbance rejection control for a buck-boost converter with load uncertainties. In: *Proceedings of 2014 33rd Chinese Control Conference*, Nanjing, China, pp. 3788-3793.

Duong, M.Q., Nguyen, V.T., Sava, G.N., Scripcariu, M., and Mussetta, M. (2017). Design and simulation of PI-type control for the Buck Boost converter. In: *Proceedings of 2017 International Conference on Energy and Environment*, Bucharest, Romania, pp. 79-82

Ghartemani, M.K., Khajehoddin, S.A., Praveen Jain, P., and Bakhshai, A. (2011). Linear quadratic output tracking and disturbance rejection. *International Journal of Control*, 84(8), pp. 1442-1449.

Ghosh, A., and Banerjee, S. (2015). Control of Switched-Mode Boost Converter by using classical and optimized Type controllers. *Control Engineering and Applied Informatics*, 17(4), pp. 114-125.

Guo, B., Hu. L., and Bai, Y. (2012). A nonlinear PID controller with tracking differentiator applying in BLDCM servo system. In: *Proceedings of 2012 7th International Power Electronics and Motion Control Conference*, Harbin, China, pp. 2467-2471.

He, G.Z., Juang, Y.T, Tsai, J.S.H., Lin, Y.Y., Guo, S.M., Shieh, L.S., and Tsai, T.J. (2017). An effective optimal linear quadratic analog tracker for the system with unknown disturbances. In: *Proceedings of 2017 IEEE 26th International Symposium on Industrial Electronics*, Edinburgh, UK, pp. 412-417.

Isayed, B.M., and Hawwa, M.A. (2007). A nonlinear PID control scheme for hard disk drive servosystems. In: *Proceedings of 2007 15th Mediterranean Conference on Control & Automation*, Athens, Greece, pp. 1-6.

Jalilvand, A., Vahedi, H., and Bayat, A. (2010). Optimal Tuning of the PID Controller for a Buck Converter Using Bacterial Foraging Algorithm. *Proceedings of IEEE International Conference on Intelligent and Advanced Systems*, Kuala Lampur, Malaysia, pp. 1-5.

Kapat, S., and Krein, P.T. (2010). Formulation of PID control for dc-dc converters based on capacitor current: A geometric context. In: *Proceedings of 12th IEEE Workshop on Control and Modeling for Power Electronics*, Boulder, USA, pp. 1-6.

Kapat, S., and Krein, P.T. (2012). Improved Time Optimal Control of a Buck Converter Based on Capacitor Current. *IEEE Transactions on Power Electronics*. 27(3), pp. 1444-1454.

Kapat, S., and Krein, P.T. (2012). Formulation of PID Control for DC–DC Converters based on Capacitor Current: A Geometric Context. *IEEE Transactions on Power Electronics*, 27(3), pp. 1424-1432.

Karanjkar, D.S., Chatterji, S., and Kumar, A. (2014). Development of linear quadratic regulator based PI controller for maximum power point tracking in solar photo-voltaic system. In: *Proceedings of 2014 Recent Advances in Engineering and Computational Sciences*, Chandigarh, India, pp. 1-6.

Kiumarsi, B., Lewis, F.L., Naghibi-Sistani, M.B., and Karimpour, A. (2015). Optimal Tracking Control of

Unknown Discrete-Time Linear Systems Using Input-Output Measured Data. *IEEE Transactions on Cybernetics*, 45(12), pp. 2770 – 2779.

Kumar, A., Vempati, A.S., Behera, L. (2013). T-S fuzzy model based Maximum Power Point Tracking control of photovoltaic system. In: *Proceedings of 2013 IEEE International Conference on Fuzzy Systems*, Hyderabad, India, pp. 1-8.

Lakshmi, S., and Raja, T.S.R. (2014). Design and implementation of an observer controller for a buck converter. *Turkish Journal of Electrical Engineering and Computer Sciences*, 22(3), pp. 562-572.

Lee, B.S., Kim, S.K., Park, J.H., and Lee, K.B. (2016). Adaptive output voltage tracking controller for uncertain DC/DC boost converter. *International Journal of Electronics*, 103(6), pp. 1002-1017.

Lewis, F.L., Vrabie, D., and Syrmos, V.L. (2012). *Optimal Control*. John Wiley and Sons, New Jersey, USA.

Lian, K.Y., Liu, C.H., and Chiu, C.S. (2017). Robust Fuzzy Output Regulator Design for Nonlinear Systems without Virtual Desired Variable Calculation. *Control Engineering and Applied Informatics*, 19(1), pp. 27-36.

Lindiya, A., Palani, S., and Iyyappan. (2012). Performance comparison of various controllers for DC-DC Synchronous Buck Converter. *Procedia Engineering*, 38, pp. 2679-2693.

Lindiya, S.A., Vijayarekha. K., and Palani, S. (2016). Deterministic LQR Controller for DC-DC Buck Converter. In: *Proceedings of IEEE Biennial International Conference on Power and Energy Systems*, Bangalore, India, pp. 1-6.

Mahendran, V., and Ramabadran, R. (2016). Fuzzy-PI-based centralised control of semi-isolated FP-SEPIC/ZETA BDC in a PV/battery hybrid system. *International Journal of Electronics*, 103(11), pp. 1909-1927.

McIntyre, M.L., Mohebbi, M., and Latham, J. (2015). Nonlinear current observer for backstepping control of buck-type converters. In: *Proceedings of 2015 IEEE 16th Workshop on Control and Modeling for Power Electronics*, Vancouver, BC, Canada, pp. 1-7.

Modares, H., and Lewis, F.L. (2014). Linear Quadratic Tracking Control of Partially-Unknown Continuous-Time Systems Using Reinforcement Learning. *IEEE Transactions on Automatic Control*, 59(11), pp. 3051-3056

Mohan, N., Undeland, T.M., and Robbins, W.P. (2007). *Power electronics: converters, applications, and design*, Wiley, New Dellhi, India.

Moreira, C.O., Silva, F.A., Pinto, S.F., and Santos, M.B. (2011). Digital LQR control with Kalman Estimator for DC-DC Buck converter. In: *Proceedings of IEEE International Conference on Computer as a Tool*, Lisbon, Portugal, pp. 1-4.

Pedroso, M.D., Nascimento, C.B., Tusset, A.M., and Kaster, M. S. (2013). Performance comparison between nonlinear and linear controllers applied to a buck converter using poles placement design. In: *Proceedings of 15th IEEE European Conference on Power Electronics and Applications*, Lille, France, pp. 1-10.

Pedroso, M.D., Nascimento, C.B., Tusset, A.M., and Kaster, M.S. (2013). A Hyperbolic Tangent Adaptive PID + LQR Control Applied to a Step-Down Converter Using Poles Placement Design Implemented in FPGA. *Mathematical Problems in Engineering*, 2013, pp. 1-8.

Qi, W., Li, S., Tan, S.C., Hui, S.Y.R. (2018). Parabolic-Modulated Sliding-Mode Voltage Control of a Buck Converter. *IEEE Transactions on Industrial Electronics*, 65(1), pp. 844 – 854.

Ruderman, M., Krettek, J., Hoffmann, F., and Bertram, T. (2008). Optimal State Space Control of DC Motor. In: *Proceedings of the 17th World Congress. The International Federation of Automatic Control*, Seoul, Korea, pp. 5796-5801.

Saleem, O., Hassan, H., Khan, A., and Javaid, U. (2017). Adaptive Fuzzy-PD Tracking Controller for Optimal Visual-Servoing of Wheeled Mobile Robots. *Control Engineering and Applied Informatics*, 19(3), pp. 56-68.

Saleem, O., and Omer, U. (2017). EKF-based self-regulation of an adaptive nonlinear PI speed controller for a DC motor. *Turkish Journal of Electrical Engineering and Computer Sciences*, 25(5), pp. 4131 – 4141.

Seraji, H. (1998). A new class of non-linear PID controller with robotic applications. *Journal of Robotic Systems*, 15, pp. 161-181.

Seshagiri, S., Block, E., Larrea, I., Soares, L. (2016). Optimal PID Design for Voltage Mode Control of DC-DC Buck Converters. In: *Proceedings of IEEE Indian Control Conference*, Hyderabad, India, pp. 99-104.

Spinu, V., Lisi, S., and Lazar, M. (2014). Constrained reference tracking for a high-speed buck converter. In: *Proceedings of 2014 IEEE Conference on Control Applications*, Juan Les Antibes, France, pp. 1255-1260.

Tahri, F., Tahri, A., Allali, A., and Flazi, S. (2012). The Digital Self-Tuning Control of a Step Down DC-DC Converter. *Acta Polytechnica Hungarica*, 9(6), pp. 49-64.

Tan, G.Q., Chen, Y.H., and Gu, L. (2014). LQR Based Optimal PID Control for Buck Converter. *Applied Mechanics and Materials*, 687-691, pp. 3221-3226.

Zhu, D., Liu, L., Liu, C. (2014). Optimal fractional-order PID control of chaos in the fractional-order BUCK converter. In: *Proceedings of 2014 IEEE 9th Conference on Industrial Electronics and Applications*, Hangzhou, China, pp. 787-791.